HHS Public Access

Author manuscript

Adv Healthc Mater. Author manuscript; available in PMC 2017 February 13.

Published in final edited form as:

Adv Healthc Mater. 2015 October ; 4(14): 2090–2099. doi:10.1002/adhm.201500403.

Combination Growth Factor Therapy via Electrostatically Assembled Wound Dressings Improves Diabetic Ulcer Healing *In Vivo*

Dr. Benjamin D. Almquist,

Department of Bioengineering Imperial College London London SW7 2AZ, UK; Koch Institute for Integrative Cancer Research Massachusetts Institute of Technology Cambridge, MA 02139, USA; Department of Chemical Engineering Massachusetts Institute of Technology Cambridge, MA 02139, USA; Institute for Soldier Nanotechnologies Massachusetts Institute of Technology Cambridge, MA 02139, USA

Steven A. Castleberry,

Koch Institute for Integrative Cancer Research Massachusetts Institute of Technology Cambridge, MA 02139, USA; Department of Chemical Engineering Massachusetts Institute of Technology Cambridge, MA 02139, USA; Institute for Soldier Nanotechnologies Massachusetts Institute of Technology Cambridge, MA 02139, USA

Julia B. Sun,

Koch Institute for Integrative Cancer Research Massachusetts Institute of Technology Cambridge, MA 02139, USA; Department of Chemical Engineering Massachusetts Institute of Technology Cambridge, MA 02139, USA; Institute for Soldier Nanotechnologies Massachusetts Institute of Technology Cambridge, MA 02139, USA

Alice Y. Lu, and

Koch Institute for Integrative Cancer Research Massachusetts Institute of Technology Cambridge, MA 02139, USA; Department of Chemical Engineering Massachusetts Institute of Technology Cambridge, MA 02139, USA; Institute for Soldier Nanotechnologies Massachusetts Institute of Technology Cambridge, MA 02139, USA

Prof. Paula T. Hammond

Koch Institute for Integrative Cancer Research Massachusetts Institute of Technology Cambridge, MA 02139, USA; Department of Chemical Engineering Massachusetts Institute of Technology Cambridge, MA 02139, USA; Institute for Soldier Nanotechnologies Massachusetts Institute of Technology Cambridge, MA 02139, USA

Abstract

Chronic skin ulcerations are a common complication of diabetes mellitus, affecting up to one in four diabetic individuals. Despite the prevalence of these wounds, current pharmacologic options for treating them remain limited. Growth factor-based therapies have displayed a mixed ability to

Correspondence to: Paula T. Hammond.

Supporting Information

Supporting Information is available from the Wiley Online Library or from the author.

drive successful healing, which may be due to non-optimal delivery strategies. Here we describe a method for coating commercially available nylon dressings using the Layer-by-Layer (LbL) process to enable both sustained release and independent control over the release kinetics of VEGF and PDGF-BB. We show that the use of strategically spaced diffusion barriers formed spontaneously by disulfide bonds enables independent control over the release rates of incorporated growth factors, and that *in vivo* these dressings improve several aspects of wound healing in db/db mice.

Keywords

layer-by-layer; electrostatic assembly; chronic wound healing; diabetic ulcer; growth factor

1. Introduction

Chronic foot ulcerations affect approximately 25% of the diabetic population[1]. These wounds are generally painful and lead to a significant decline in quality of life[2]. While a variety of options are available to treat these wounds, many are inefficient when used in isolation due to a diverse combination of causative factors including mechanical stress, chronic inflammation, neuropathy, ischemia, and innate biomolecular changes[3]. Because of this complexity, it is often challenging to promote full wound resolution, leaving the door open for opportunistic infections that set the stage for a downward spiral leading to amputation.

In order to increase the overall probability of wound closure and reduce the progression to more serious complications, there is a need for efficient strategies to address each of the factors that contribute to the formation of a chronic wound. While factors such as mechanical stress can be effectively addressed using offloading orthotics[3a], methods for addressing other contributing factors including neuropathy, ischemia, and chronic inflammation are much less successful. Many times these other factors lead to dysregulation of the cell signaling that normally occurs during the healing of acute wounds in healthy individuals[3c, 4]. In these healthy wounds, combinations of growth factors and cytokines are released to coordinate the behavior of cells involved in the repair process[5]. However, in diabetic individuals these signals are commonly disrupted and contribute to the formation of chronic ulcerations[3c, 4].

This disruption in signaling has been a motivating factor for attempting to use exogenous growth factors as a means to spur tissue repair[6]. Unfortunately, despite many promising candidates only a small fraction of growth factors have been successfully translated to clinics around the world. Examples of these include platelet-derived growth factor BB (PDGF-BB) in the USA and fibroblast growth factor 2 (FGF-2) in China and Japan. However in the case of PDGF-BB, the currently approved formulation carries concerns regarding both the efficacy and safety and has been given a ‘black box’ warning by the FDA[7].

The poor efficacy and safety issues of growth factor-based therapeutics likely arise in part due to a non-optimal delivery strategy and physiologically inappropriate dosings. In the

clinic, PDGF-BB is delivered via a carboxymethylcellulose-based gel that results in a large bolus release of growth factor upon application. Due to the short temporal persistence of PDGF-BB *in vivo* (intravenous t1/2 = 2 minutes)[8], this method of delivery requires a high concentration of growth factor to spur noticeable changes in wound healing[9]. Additionally, unlike the endogenous process of wound repair that utilizes multiple growth factors[5b, 10], PDGF-BB is delivered as a lone therapeutic, eliminating any potential beneficial interactions arising from combination therapies that may increase overall effectiveness.

In order to enable the use of multiple growth factors and break the need to use high concentrations of growth factors, we aimed to establish a new therapeutic strategy that possesses several key features: 1) the platform should have the potential to be easily integrated into platforms used in a clinical setting and 2) it should possess the ability to deliver multiple growth factors and control their delivery kinetics. We use the layer-by-layer (LbL) process to construct drug-loaded multilayer films and overcome the limitations of current growth factor-based therapeutics, establishing a flexible strategy for developing more effective treatments. LbL is an iterative self-assembly process that takes advantage of complimentary interactions (e.g. electrostatics, hydrogen bonding) to control the deposition of materials on a substrate of interest[11]. It can achieve high therapeutic loadings compared to traditional polymer blends, and due to its amenability to water-based solutions, is an ideal platform for assembling biomaterials that contain sensitive biologics including growth factors[12]. In this study, we use the LbL process to develop a flexible platform that allows the delivery of multiple growth factors from commercially available wound dressings. We establish the ability to release physiologically relevant amounts of active growth factors over approximately two weeks and evaluate the effects of combination growth factor therapy in a murine model of diabetic ulcer healing.

2. Results & Discussion

Woven nylon contact layer dressings were identified as the substrate of choice. In the clinic these dressings are generally placed in contact with wounds to act as a barrier between the wound tissue and gauze, with the mesh size of the contact layer preventing tissue growth into the gauze. Here, we coated these contact dressings via LbL to create bioactive dressings incorporating vascular endothelial growth factor 165 (VEGF) and/or PDGF-BB (Figure 1). VEGF and PDGF-BB were chosen due to their demonstrated efficacy as a pro-angiogenic therapy[13], allowing the evaluation of the LbL platform as a viable delivery strategy by targeting the common issue of limited angiogenesis in diabetic ulcers. This therapeutic strategy is based on the stimulation of vascular sprouting and vessel growth via VEGF signaling, and the subsequent stabilization of nascent vasculature by mural cells via PDGF-BB mediated recruitment[14]. While this strategy has been demonstrated in various tissue environments *in vivo*[15], the impact of soluble, controlled-release VEGF/PDGF-BB into the bed of a chronic wound has yet to be established; instead, previous work has relied on engineered matrix binding proteins for improving efficacy[16]. The chronic wound environment carries additional challenges for soluble growth factors compared to acutely healing tissues, with chronic environments displaying elevated levels of proteases and pro-inflammatory cytokines, as well as varying levels of hypoxia, all factors that lead to an

aggressive and degradative microenvironment that can reduce the effectiveness of growth factors and other protein-based therapeutics[17].

Therapeutic dressings were fabricated using a repeating tetralayer architecture that consists of hydrolytically degradable poly(β-amino esters) (Poly1 & Poly2)[18], poly(acrylic acid) (PAA), VEGF and/or PDGF-BB, and heparan sulfate (HS) (Figure 2a). The use of Poly1/Poly2 allows for control over the degradation rate of the LbL film[19], while PAA and HS have been validated in the past as a method for incorporating active growth factors into LbL dressings[20]. In the case of dermal wound healing, dressing changes are likely to occur within one to two weeks. Dressing architectures were designed for release kinetics with an exponentially decaying release of VEGF in combination with sustained release of PDGF-BB. These kinetics align with previous work establishing the optimal temporal kinetics for promoting angiogenesis with combination delivery of VEGF and PDGF-BB, and relies on VEGF driving the initial formation of new vasculature followed by maturation of the vessels via PDGF-BB-mediated mural cell recruitment[15a]. In order to achieve this temporal program, PDGF-BB-containing films were assembled in direct contact with the woven nylon substrate. VEGF-containing films were subsequently assembled on top of the PDGF-BB films in order to coordinate distinct release via surface-based erosion (Figure 2a).

The *in vitro* release profile for the VEGF/PDGF-BB dressing is shown in Figure 2b and reveals that significant interlayer diffusion occurs during the construction of the LbL film[21], resulting in a polymer blend that lacks distinct release kinetics for each growth factor. In order to reduce the propensity for interlayer blending, selectively crosslinked “barrier layers” were added to the design. This was carried out through chemical conjugation of cysteine to PAA (PAAC) using well-established EDC chemistry (average cysteine:COOH ; 1:4) in order to enable reversible crosslinking via formation of disulfide bonds. Second generation dressings were fabricated with a PAAC layer replacing PAA in every third tetralayer of the PDGF-BB section of the film and a barrier region of higher crosslinking between the PDGF-BB and VEGF sections of the film (Figure 2c). Previous studies using neutron reflectivity have shown that this spacing is sufficient to prevent blending and interaction of two distinct LbL layers[22]. Here, this periodic spacing promotes intra-layer crosslinking of the PAAC within the individually deposited layer instead of crosslinking between the different PAAC layers of the PDGF-BB section of the film, This sets up diffusion barriers that reduce the level of film blending but do not completely inhibit PDGF-BB release.

The PAAC-containing dressings were subsequently characterized to determine the impact of the barrier layers on the release behavior of VEGF and PDGF-BB. As shown in Figure 2d, the release from the top layers containing VEGF with PAA and HS is not impacted. In contrast, the kinetics of PDGF-BB release are significantly altered, with release now sustained for approximately 11 days (Figure 2d), leading to significant differences in release behavior. However, the total protein loading is not affected by the incorporation of PAAC (Table 1). In order to verify that the delayed release behavior of PDGF-BB is occurring due to the formation of intra-layer disulfide bonds, dressings were fabricated with PAA-C replacing PAA for all layers throughout the dressings (Figure S1). In these dressings, minimal protein release is observed due to extensive crosslinks formed throughout the

thickness of the film (between each individually deposited PAAC layer). The system with staggered VEGF/PDGF-BB release profile represents the more optimal release kinetics as discussed above, and was selected for further study.

While it has been previously demonstrated that growth factors incorporated into LbL films remain active[12g, 20], the introduction of free thiols throughout the PDGF-BB section of the film raises concerns regarding thiol-mediated denaturation of the encapsulated PDGF-BB. In order to verify that active PDGF-BB is being released, two *in vitro* assays were performed. First, PDGF-BB released during the first 24 hours of degradation was added to cultures of primary human dermal fibroblasts (HDF) from hyperglycemic patients, followed by measurement of PDGF Receptor β (PDGF-Rβ) phosphorylation. Significant phosphorylation was observed in cells stimulated with release solutions (33.2±14.9 ng/mL pPDGF-Rβ), while no detectable phosphorylation was found for PBS-stimulated cells. This data verifies that PDGF-BB released from dithiol-crosslinked films retains the ability to phosphorylate cognizant receptors. The second verification of PDGF-BB activity was provided in a migration assay of HDF. Degradation solutions from 12 hrs, 6.6 days, and 10.8 days were added to HDFs and the migration compared to PBS controls. In all cases, degradation solutions promoted increases in cell migration over PBS controls, and no significant difference was observed between the different degradation time points, indicating that following dressing fabrication, no functional protein degradation occurs within the dressings over the timeframe of release of approximately 11 days (Figure 3 and Figure S2 for example migration images).

Having confirmed that the dithiol-crosslinked films retain the ability to release active proteins, we next aimed to understand how the dressing impacts the process of wound repair. Owing to the fact that tissue repair is a complex biological process that is poorly recapitulated in an *in vitro* setting, a majority of characterization focused on the *in vivo* impact in db/db mice. db/db mice are a genetic model of type II diabetes, and are commonly used to explore therapeutic strategies for healing diabetic ulcers[23]. In this study, two full thickness skin wounds (through the panniculus carnosus) were made on the backs of mice.

Wounds were covered with either control dressings (bare nylon substrate), dressings containing both VEGF and PDGF-BB (average VEGF dose: 93±25 ng; average PDGF-BB dose: 43±15ng), or dressings containing either VEGF or PDGF-BB that possess the same individual release kinetics and dosage level as found in the combination dressing (Figure 2d and Figure S3). A transparent adhesive dressing was then applied over the wound to hold the therapeutic dressing in place and prevent infection. Wound evaluation at Day 7 and Day 14 reveals significant qualitative and quantitative differences between the treatment regimens. Gross examination of the wounds shows overall changes to the visual appearance of the wounds (Figure 4). Control wounds and those treated with only VEGF tend to appear overall lighter in color than PDGF-BB and combination dressings one week after surgery. In the latter cases, the deeper red granulation tissue appears to align with the characteristics of wound that is healing properly; the deeper red color is likely due to a higher density of blood vessels, and is characteristic of healthy, vascularized tissue[24]. Quantifying the extent of vessel growth via immunofluorescence labeling of CD31 indicates a significant increase in vascular density in the VEGF/PDGF-BB combination treated wounds compared to control

wounds and those treated with only VEGF (Figure 5), along with the combination treatment leading to the highest maximum density of vessels in the wound tissue that we observed at week one. The staining of α-smooth muscle actin shows limited maturation of the vessels by mural cells at week one, although there is evidence of the maturation process beginning in the wounds undergoing the combination treatment. By two weeks after surgery the wounds treated with any of the growth factor therapies exhibit an increase in angiogenesis compared to the untreated control wounds. However, the combination treatment has the highest average vessel density and a maximum vessel density approximately twice that of any other treatment, in agreement with previous work demonstrating the benefit of the VEGF/PDGF-BB treatment. These combination-treated wounds also display a high number of mural cells surrounding the vessels, indicating that a robust, mature vascular system is being generated.

Having established that the combination therapy conveys the largest improvement in vascularization within the wound bed, we next aimed to establish how the different therapeutic strategies affect various processes specific to wound healing. One such process is the formation of granulation tissue within the wound[25]. This temporary tissue is critical for establishing a matrix that enables reepithilialization, helps reduce infection, and provides a means for healing via secondary and tertiary intention (two methods of wound healing that involve the formation of significant quantities of granulation tissue to heal the wound). In prior research, PDGF-BB has been shown to spur the growth of granulation tissue, however the authors of that work used greater than 300 times the amount of PDGF-BB contained in the dressings used here[26]. Adding to this information is the fact that PDGF-BB has been shown to possess a strong dose-dependent efficacy[9], making it unclear as to how effective the bioactive dressings would be at promoting the growth of granulation tissue. It should be noted, though, that engineering proteins to increase their matrix retention lifetimes have demonstrated efficiency at lower levels of protein[16], suggesting that the controlled release strategy used here may be a promising approach.

To quantify the amount of granulation tissue within each wound, serial tissue sections were taken every 250–500um through the entirety of the wounds. The average thickness of granulation tissue for each tissue section was measured and the average thickness across the wounds determined. At one week, the combination dressings are the only treatment to display on average a significant increase in granulation tissue over the control wounds (Figure 6). This trend continues at week two, with only the combination dressing differentiating itself from control treated wounds. At this point, the average thickness of the granulation tissue in the mice undergoing the combination treatment is equivalent to the average skin thickness (0.59±0.09mm), meaning this new temporary tissue completely fills the wound site. Wounds treated with only PDGF-BB do not display an increase in granulation tissue; these results demonstrate that the strategy of combining growth factors that generate cooperative benefits may be a viable strategy for improving both the translational effectiveness of growth factors while simultaneously reducing the required dosage levels. Here, the interaction that gives rise to formation of additional granulation tissue is likely the higher level of angiogenesis in the combination treated wounds. Previous studies have shown that expression of dominant-negative VEGF Receptor-2 in the wounds of mice results in lower levels of wound angiogenesis and reduced amounts of granulation tissue[27]. Furthermore, poorly vascularized wounds in the clinic are commonly found to be

poor healers[27–28]. Taken together, these results suggest that the increased growth and stabilization of new vessels within the granulation tissue due to beneficial interactions of VEGF and PDGF-BB signaling supports an overall increase in amount of granulation tissue at day 7 and 14.

Combining the findings from both the angiogenesis and granulation tissue measurements, it is highly likely that differing levels of cellular proliferation exist within the wound bed. Immunohistochemistry examination of the fraction of Ki-67 expressing cells within the granulation tissue confirms that combination VEGF/PDGF-BB therapy leads to an overall higher fraction of proliferating cells than the other treatment groups, with 31.2±4.8% of cells positive for Ki-67 compared to 22.4±2.9%, 20.5±4.9%, and 9.6±7.3% for VEGF only treatment, PDGF-BB only treatment, and untreated controls, respectively (Figure 7). Taking this data together with the angiogenesis and granulation tissue measurements indicate that the benefits of combination therapy with VEGF with PDGF-BB include enhancing the overall degree of cellular proliferation in the wound bed over PDGF-BB used in isolation.

In order to gain more insight into the granulation tissue that forms following each treatment regime, a rough estimate of the ratio of thick to thin collagen fiber deposition was determined via picrosirius red staining. Picrosirius red stain enhances the natural birefringence of fibrillar collagen, allowing easy quantification under cross-polarized light[29]. The color undergoes a shift from green to yellow-orange as collagen fibrils increase in thickness, allowing differentiation between thin and thick collagen fibers (Figure S4). The thick fiber category generally consists of collagen I fibers, while the thin fiber category contains the collagen III signal, immature collagen I fibers, and collagen I fibers altered during histological processing. Here the ratio of thick to thin fibers within the granulation tissue does not vary significantly between treatment groups, signifying that at a given time after treatment the collagen within the tissue is similar (Table 2). Furthermore, as the wounds heal, the thick to thin ratio increases; this trend is in good agreement with the previous observations of the collagen fiber ratio in healing wounds[30], indicating that the growth factors used here do not cause dramatic alterations in the distribution of collagen within the granulation tissue. This is not unexpected as the ratios of collagen types are closely linked with the levels of proteases within the tissue microenvironment, and none of the growth factors used here are anticipated to shift these levels towards a substantially different proteolytic microenvironment.

One function of this newly formed granulation tissue is to promote wound closure, both through myofibroblast-mediated contraction and providing a substrate for reepithilialization[25]. The amount of wound contraction was determined by measuring the closure of the panniculus carnosus muscle, which is cut through during full-thickness skin wounding and does not regenerate over the course of the study, while the overall rate of closure was determined by the remaining defect in the epidermis. In each case, areal measurements from serial wound sections are used to determine the degree of healing. At one week, wounds treated with the combination dressings display an increased rate of wound contraction, although this difference disappears by week two (Figure 8a,b). The exact mechanism behind the increased contraction at week one is currently unknown and under further investigation. The standard mechanism of myofibroblast-mediated contraction is a

possibility, although the amount of granulation tissue present at this time point is not thought to be sufficient to drive contraction.

The overall rate of wound closure, measured by the size of the remaining defect in the epidermis, shows no difference between the treatments at one or two weeks post wounding (Figure 8c,d). This result is not unexpected, since neither VEGF nor PDGF-BB are motogenic towards keratinocytes but instead expressed by keratinocytes as paracrine signals for cells in the underlying granulation tissue[5b, 31]. While VEGF has been shown to increase the rate of wound closure in other experiments[32], those results use significantly more growth factor than used here. In that case VEGF is suggested to increase the recruitment of bone marrow-derived cells and alter expression of various growth factors including PDGF and FGF2. Here, we do not find indications of sufficient modulation of these growth factor networks to increase the rate of wound closure. Increasing the dosage of PDGF-BB is not likely to alter this finding, as significantly higher doses of PDGF-BB have been found to simply promote the formation of granulation tissue and not drive reepithilialization[26]. Furthermore, increasing the dosage of VEGF is likely not a translatable strategy, as large doses of VEGF promote vascular permeability, bleeding, and the subsequent formation of disordered vasculature[33]. Instead, the addition of the mesenchymally derived growth factor fibroblast growth factor-7 (FGF-7) may stimulate the migration of epidermal keratinocytes over the newly formed granulation tissue[31]. In addition, hepatocyte growth factor (HGF) may be an interesting target for increasing the rate of epithelialization, as c-met signaling has been shown to play an important role in keratinocyte migration[34]. In either case, the flexibility of this LbL dressing allows for easy adaptation to include these additional bioactive factors that, in conjunction with the VEGF/PDGF-BB therapy, may provide a comprehensive combinatorial strategy that drives the multifaceted process of wound repair.

3. Conclusion

Bioactive dressings assembled using the LbL process provide a means for controlling the delivery of multiple active growth factors that are implicated in the process of wound repair. These dressings dramatically reduce the amount of growth factor necessary for improved functional outcomes and do not require the use of modified proteins, laying the foundation for both an exploratory platform for investigative research and a translational modality for potential therapeutic strategies. As a proof of concept, combination dressings containing VEGF and PDGF-BB were fabricated and evaluated using a murine model of chronic wound healing. In addition to promoting angiogenesis, this combination of growth factors also promotes significant increases in the formation of granulation tissue and/or cellular proliferation when compared to dressings utilizing single growth factor therapeutics. More broadly, the dressings used here achieve these results at protein levels between 300 and 700 times lower than traditional delivery methods, and at comparable protein levels to the newest strategies involving designer protein constructs[16,26].

4. Experimental Section

4.1 Materials

Polyacrylic acid (Mw 1,000,000) was obtained from Polysciences, Inc. (Warrington, PA). Poly (β-amino ester) 1 and 2 (Poly1 and Poly2) were synthesized as previously described[18]. Heparan sulfate (Mw 14.6 kDa) was obtained from Celsus Laboratories, Inc. (Cincinnati, OH). 5,5'-Dithiobis(2-nitrobenzoic acid) (Ellman's Reagent, BioReagent) and L-Cysteine (BioUltra) were obtained from Sigma-Aldrich (St. Louis, MO). Sulfo-NHS and EDC were obtained from Thermo Fisher Scientific (Waltham, MA). Sodium acetate buffer (3 M) was obtained from Sigma Aldrich. Carrier-free PDGF-BB and VEGF-165 were obtained from BioLegend, Inc. (San Diego, CA). PDGF-BB and VEGF-165 Duoset ELISA kits and phospho-PDGF-Rβ ELISA kits were obtained from R&D Systems (Minneapolis, MN). Oris cell migration assays were obtained from Platypus Technologies (Madison, WI). Tegaderm woven nylon wound dressings and adhesive dressings were obtained from 3M (Minneapolis, MN). Rat anti-mouse CD31 antibody (MEC 13.3 clone, 553370) was obtained from BD Biosciences (San Jose, CA). Goat anti-mouse α-smooth muscle actin antibody (PA5-18292) was obtained from Thermo Fisher Scientific Inc. Chicken anti-rat Alexa488 (A21470) and chicken anti-goat Alexa594 (A21468) were obtained from Life Technologies. Rabbit anti-mouse Ki-67 (ab16667) was obtained from Abcam (Cambridge, MA). Chicken serum (16110-082) was obtained from Life Technologies. Proteinase K (17916) was obtained from Thermo Fisher Scientific Inc. DAPI and Prolog Gold antifade reagent were obtained from Life Technologies. Primary human dermal fibroblasts were a gift from Dr. Aristidis Veves (Joslin-Beth Israel Deaconess Foot Center). db/db mice were obtained from The Jackson Laboratory (strain: BKS.Cg-Dock 7^{m} +/+ $Lepr^{db}$/J).

4.2 PAA-Cysteine Conjugation

Briefly, EDC and Sulfo-NHS were added at a ratio of 1:2 to a 3g/L PAA solution in 0.5 M NaCl and allowed to react for 25 minutes at pH 6.0. 2-mercaptoethanol was then added and the pH adjusted 7.0. L-cysteine was then added to a final concentration of 3g/L and allowed to react for 3 hours. The resulting solution was subsequently dialyzed in decreasing concentrations of acidic NaCl over the course of 3 weeks using dialysis tubing with a MWCO=50,000. The resulting solution was lyophilized to obtain the purified PAAC. Ellman's reagent was then used to determine the degree of PAA conjugation following reduction of disulfide bonds in the PAAC using tris-(2-carboxyethyl)phosphine.

4.3. Preparation of Polyelectrolyte Dipping Solutions

Linear poly(ethlyeneimine) (LPEI) solutions were prepared as 10mM solutions using deionized water, pH 4.25. Polystyrene sulphonate (PSS) solutions were prepared as 10mM solutions using deionized water, pH 4.75. Poly1, Poly2, heparan sulfate, PAA, and PAA-C dipping solutions were prepared as 2mg/mL solutions in 100mM sodium acetate buffer, pH 5.0, 0.2 μm filtered. PDGF-BB and VEGF dipping solutions were prepared as 50μg/3mL solutions in 100mM sodium acetate buffer, pH 5.0, 0.2 μm filtered. All wash baths were 100mM sodium acetate, pH 5.0 except for use with LPEI and PSS, which were washed with DI water at a pH corresponding to the respective dipping solution.

4.4. Film Construction

Woven nylon dressings were precut with a 6mm diameter biopsy punch prior to dipping. Dressings were attached to a custom dipping arm for a Carl Zeiss HMS programmable slide stainer and oxygen plasma treated for 5 minutes in pure oxygen. Immediately following plasma treatment, ten LPEI/PSS bilayers were deposited to form a nondegradable baselayer of uniform charge using a dipping cycle of 5 minutes per polymer solution followed by two one minute washes in DI water. Following the baselayer coating process, dressings were dipped using a repeating tetralayer architecture of Poly1 or Poly 2, PAA or PAA-C, PDGF-BB or VEGF, and heparan sulfate (Figure 2). All polymer solutions were dipped for 5 minutes followed by two washes of one minute each. Growth factor solutions were dipped for 10 minutes followed by a single wash step of 10 seconds. PDGF-BB containing film was deposited following the baselayer step, with VEGF containing film subsequently deposited on top of the PDGF-BB film. In dressings that contained only one growth factor, the other growth factor was replaced with either Poly1 or Poly2 depending on which Poly was being used in that tetralayer. All solutions were changed when a new section of the films were started (e.g. PDGF-BB section, VEGF section). Each section of the films (VEGF or PDGF-BB) contained 40 tetralayer repeats, while the highly crosslinked barrier between VEGF and PDGF-BB sections in the PAAC dressings contained 5 bilayer repeats of PAAC and Poly2.

4.5 In Vitro Release Profiles and Growth Factor Loading

Film-coated dressings were placed in sterile microcentrifuge tubes containing 1 mL of sterile PBS and carried out at 37°C. At each timepoint, dressings were removed from their current tubes and placed into new microcentrifuge tubes. The release solutions were aliquoted and frozen. Degradations were carried out over the course of two weeks. Degradation solutions were subsequently characterized via ELISA to determine the average release profiles and total growth factor loading. Each timepoint was measured in duplicate and at least 3 different dressings were used to determine the release profiles and average growth factor loadings.

4.6 Growth Factor Activity Assays

HDFs were cultured in DMEM with 5% FBS, 1% antibiotic-antimycotic, and 2 mM L-glutamine. PDGF-Rβ phosphorylation ELISA and cell migration assays were carried out according to the manufacturers instructions. Briefly, for the phosphorylation assays cells were grown to 80% confluence and serum starved for 8 hours. Dressing degradation solution or PBS was added to the cultures to a final PDGF-BB concentration of 5ng/mL. Stimulation was allowed to occur for 15 minutes, followed by washing and cell lysis. Lysates were then analyzed via ELISA. For the cell migration assays, HDFs were seeded in the Oris cell migration plate and cultured for 12 hours. Stoppers were removed and cells washed. Serum-free media with either release solutions from various timepoints or PBS was added to the cells and incubated for 12 hours. PDGF-BB concentration was normalized to 420pg/mL for each timepoint. Cells were then fixed, stained with DAPI, and the extent of cell migration measured.

4.7 In Vivo Dressing Evaluation

All animal work was performed in accordance with protocols approved by the Committee on Animal Care at the Massachusetts Institute of Technology. Female db/db mice were obtained at 8 weeks of age and were 10–12 weeks old at the time of surgery. Daily blood glucose measurements were used to confirm the onset of diabetes, which was defined as 10 continuous days with blood glucose levels above 300mg/dL. Three to five days prior to surgery, hair on the dorsum of db/db mice was removed using a depilatory cream. Immediately prior to surgery, mice were anesthetized with 1–3% isofluorane and given 0.1 mg/kg analgesics (Buprenex). The skin was prepared with chlorhexidine and two 6mm full-thickness skin wounds were made off mid-line using biopsy punches. Coated dressings or bare control dressings were placed directly on the wounds. Coated dressings were fabricated immediately prior to surgery, with no sterilization protocols used following fabrication due to skin wounds being non-sterile. The therapeutic dose was chosen to be inline with other recent reports[16]. The wounds were then covered with adhesive Tegaderm to hold the dressings in place and reduce the chance of infection. Body weights were measured daily to ensure no mice were included in analysis that lost greater than 10% of their body weight following surgery. Wounds displaying overt signs of infection were also excluded from the study. One and two weeks after surgery, mice were euthanized and the wound tissues taken for histological analysis. For all animal experiments, final group sizes were n=5–8.

4.8 Histology

Wound tissue was fixed in formalin-free zinc fixative for 48 hours. The wounds were subsequently embedded in paraffin and serial sections taken every 250μm through the entirety of the wound. H&E staining was done at each level and used to make 2-D reconstructions of the wound. Wound size and panniculus carnosus gap were measured using area measurements from these 2-D reconstructions. Granulation tissue area was manually isolated and measured for each section and the average area across the wound determined. Unstained slides were taken at each level for immunohistochemistry (IHC) and picrosirius staining. IHC staining of CD31 and α-SMA were carried out with primary antibody concentrations of 1:100 and 1:200, respectively. Secondary antibody staining was done at a concentration of 1:500. Ki67 staining was done at an antibody concentration of 1:100. All measurements were carried out using ImageJ.

4.9 Statistics

For normally distributed data sets with equal variances, one-way ANOVA testing followed by a Tukey post-hoc test was carried out across groups. For normal data sets with unequal variances, a Welch test was performed followed by Games-Howell post-hoc testing. In cases that required non-parametric evaluation, a Kruskal-Wallis ANOVA was carried out and followed by Steel-Dwass post-hoc testing. In all cases, significance was defined as p 0.05. Outliers were identified using the outlier labeling rule with k=2.4. A Grubbs outlier test with α=0.01 was then used on identified outlier candidates to confirm outliers for exclusion. For all animal experiments, each group n=5–8. Statistical analysis was carried out using SPSS, JMP, and Excel.

Supplementary Material

Refer to Web version on PubMed Central for supplementary material.

Acknowledgments

JBS and SAC contributed equally to this work. This research was supported in part by funding and core facilities provided by the U.S. Army Research Office under contract W911NF-07-D-0004 at the MIT Institute of Soldier Nanotechnology and by funding from the Sanofi-Aventis and MIT Center for Biomedical Innovation. BDA acknowledges postdoctoral fellowship support from the National Institutes of Health under Ruth L. Kirschstein National Research Service Award F32-DK097858. The contents of this work are solely the responsibility of the authors and do not necessarily represent the official views of the NIDDK or NIH. We thank the MIT Koch Institute Swanson Biotechnology Center, which is supported by the Koch Institute Core Grant P30-CA14051 from the NCI, for the use of facilities and specifically the Hope Babette Tang (1983) Histology Facility. We also thank the W.M. Keck Microscopy Facility at the Whitehead Institute for Biomedical Research.

References

1. a) Fonder MA, Lazarus GS, Cowan DA, Aronson-Cook B, Kohli AR, Mamelak AJ. J Am Acad Dermatol. 2008; 58:185. [PubMed: 18222318] b) Sen CK, Gordillo GM, Roy S, Kirsner R, Lambert L, Hunt TK, Gottrup F, Gurtner G, Longaker MT. Wound Repair Regen. 2009; 17:763. [PubMed: 19903300] c) Falanga V. Lancet. 2005; 366:1736. [PubMed: 16291068]
2. Vileikyte L. Diabetes/Metab Res Rev. 2001; 17:246.
3. a) Cavanagh PR, Lipsky BA, Bradbury AW, Botek G. Lancet. 2005; 366:1725. [PubMed: 16291067] b) Game FL, Hinchliffe RJ, Apelqvist J, Armstrong DG, Bakker K, Hartemann A, Löndahl M, Price PE, Jeffcoate WJ. Diabetes/Metab Res Rev. 2012; 28(s1):119.c) Medina A, Scott PG, Ghahary A, Tredget EE. J Burn Care Rehabil. 2005; 26:306. [PubMed: 16006837]
4. Blakytny R, Jude E. Diabetic Med. 2006; 23:594. [PubMed: 16759300]
5. a) Singer AJ, Clark RAF. N Engl J Med. 1999; 341:738. [PubMed: 10471461] b) Werner S, Grose R. Physiol Rev. 2003; 83:835. [PubMed: 12843410] c) Broughton G II, Janis JE, Attinger CE. Plast Reconstr Surg. 2006; 117:12S. [PubMed: 16799372]
6. a) Bennett SP, Griffiths GD, Schor AM, Leese GP, Schor SL. Br J Surg. 2003; 90:133. [PubMed: 12555288] b) Pierce GF, Mustoe TA. Annu Rev Med. 1995; 46:467. [PubMed: 7598479]
7. Food and Drug Administration, Silver Spring, MD 2008
8. Bowen-Pope DF, Malpass TW, Foster DM, Ross R. Blood. 1984; 64:458. [PubMed: 6331547]
9. Wieman TJ, Smiell JM, Su Y. Diabetes Care. 1998; 21:822. [PubMed: 9589248]
10. a) Martin P. Science. 1997; 276:75. [PubMed: 9082989] b) Schreml S, Szeimies RM, Prantl L, Landthaler M, Babilas P. J Am Acad Dermatol. 2010; 63:866. [PubMed: 20576319]
11. Decher G. Science. 1997; 277:1232.
12. a) Boudou T, Crouzier T, Ren K, Blin G, Picart C. Adv Mater. 2010; 22:441. [PubMed: 20217734] b) Tang Z, Wang Y, Podsiadlo P, Kotov NA. Adv Mater. 2006; 18:3203.c) Pavlukhina S, Sukhishvili S. Adv Drug Delivery Rev. 2011; 63:822.d) Crouzier T, Ren K, Nicolas C, Roy C, Picart C. Small. 2009; 5:598. [PubMed: 19219837] e) Vrana NE, Erdemli O, Francius G, Fahs A, Rabineau M, Debry C, Tezcaner A, Keskin D, Lavalle P. J Mater Chem. 2014; 2:999.f) Dierich A, Le Guen E, Messaddeq N, Stoltz JF, Netter P, Schaaf P, Voegel JC, Benkirane-Jessel N. Adv Mater. 2007; 19:693.g) Shah NJ, Hyder MN, Moskowitz JS, Quadir MA, Morton SW, Seeherman HJ, Padera RF, Spector M, Hammond PT. Sci Transl Med. 2013; 5:191ra83.h) Picart C. Curr Med Chem. 2008; 15:685. [PubMed: 18336282]
13. a) Richardson TP, Peters MC, Ennett AB, Mooney DJ. Nat Biotechnol. 2001; 19:1029. [PubMed: 11689847] b) Chen RR, Silva EA, Yuen WW, Mooney DJ. Pharm Res. 2007; 24:258. [PubMed: 17191092]
14. a) Jain RK. Nat Med. 2003; 9:685. [PubMed: 12778167] b) Herbert SP, Stainier DYR. Nat Rev Mol Cell Biol. 2011; 12:551. [PubMed: 21860391] c) Carmeliet P, Jain RK. Nature. 2011; 473:298. [PubMed: 21593862]

15. a) Hao X, Silva EA, Månsson-Broberg A, Grinnemo KH, Siddiqui AJ, Dellgren G, Wärdell E, Brodin LÅ, Mooney DJ, Sylvén C. Cardiovasc Res. 2007; 75:178. [PubMed: 17481597] b) De la Riva B, Sánchez E, Hernández A, Reyes R, Tamimi F, López-Cabarcos E, Delgado A, Évora C. J Controlled Release. 2010; 143:45.c) Lutton C, Young YW, Williams R, Meedeniya ACB, Mackay-Sim A, Goss B. J Neurotrauma. 2012; 29:957. [PubMed: 21568693]
16. a) Martino MM, Tortelli F, Mochizuki M, Traub S, Ben-David D, Kuhn GA, Müller R, Livne E, Eming SA, Hubbell JA. Sci Transl Med. 2011; 3:100ra89.b) Martino MM, Briquez PS, Güç E, Tortelli F, Kilarski WW, Metzger S, Rice JJ, Kuhn GA, Müller R, Swartz MA, Hubbell JA. Science. 2014; 343:885. [PubMed: 24558160]
17. Yager DR, Nwomeh BC. Wound Repair Regen. 1999; 7:433. [PubMed: 10633002]
18. Lynn DM, Langer R. J Am Chem Soc. 2000; 122:10761.
19. Smith RC, Leung A, Kim BS, Hammond PT. Chem Mater. 2009; 21:1108. [PubMed: 20161308]
20. a) Macdonald ML, Rodriguez NM, Shah NJ, Hammond PT. Biomacromolecules. 2010; 11:2053. [PubMed: 20690713] b) Shah NJ, Macdonald ML, Beben YM, Padera RF, Samuel RE, Hammond PT. Biomaterials. 2011; 32:6183. [PubMed: 21645919] c) Crouzier T, Szarpak A, Boudou T, Auzély-Velty R, Picart C. Small. 2010; 6:651. [PubMed: 20155753]
21. a) Uhlig K, Madaboosi N, Schmidt S, Jäger MS, Rose J, Duschl C, Volodkin DV. Soft Matter. 2012; 8:11786.b) Vogt C, Ball V, Mutterer J, Schaaf P, Voegel JC, Senger B, Lavalle P. J Phys Chem B. 2012; 116:5269. [PubMed: 22486371]
22. Lösche M, Schmitt J, Decher G, Bouwman WG, Kjaer K. Macromolecules. 1998; 31:8893.
23. a) Davidson JM. Arch Dermatol Res. 1998; 290:S1. [PubMed: 9710378] b) Tsuboi R, Shi CM, Rifkin DB, Ogawa H. J Dermatol. 1992; 19:673. [PubMed: 1293153]
24. Bates DO, Pritchard Jones RO. Int J Low Extrem Wounds. 2003; 2:107. [PubMed: 15866835]
25. Baum CL, Arpey CJ. Dermatol Surg. 2005; 31:674. [PubMed: 15996419]
26. Chan RK, Liu PH, Pietramaggiori G, Ibrahim SI, Hechtman HB, Orgill DP. J Burn Care Res. 2006; 27:202. [PubMed: 16566566]
27. Tsou R, Fathke C, Wilson L, Wallace K, Gibran N, Isik F. Wound Repair Regen. 2002; 10:222. [PubMed: 12191004]
28. Stadelmann WK, Digenis AG, Tobin GR. Am J Surg. 1998; 176(Suppl 2A):39S.
29. Rich L, Whittaker P, Braz. J Morphol Sci. 2005; 22:97.
30. a) Junge K, Klinge U, Klosterhalfen B, Mertens PR, Rosch R, Schachtrupp A, Ulmer F, Schumpelick V. J Invest Surg. 2002; 15:319. [PubMed: 12542866] b) Cuttle L, Nataatmadja M, Fraser JF, Kempf M, Kimble RM, Hayes MT. Wound Repair Regen. 2005; 13:198. [PubMed: 15828945]
31. Werner S, Krieg T, Smola H. J Invest Dermatol. 2007; 127:998. [PubMed: 17435785]
32. Galiano RD, Tepper OM, Pelo CR, Bhatt KA, Callaghan M, Bastidas N, Bunting S, Steinmetz HG, Gurtner GC. Am J Pathol. 2004; 164:1935. [PubMed: 15161630]
33. Dor Y, Djonov V, Abramovitch R, Itin A, Fishman GI, Carmeliet P, Goelman G, Keshet E. EMBO J. 2002; 21:1939. [PubMed: 11953313]
34. Chmielowiec J, Borowiak M, Morkel M, Stradal T, Munz B, Werner S, Wehland J, Birchmeier C, Birchmeier W. J Cell Biol. 2007; 177:151. [PubMed: 17403932]

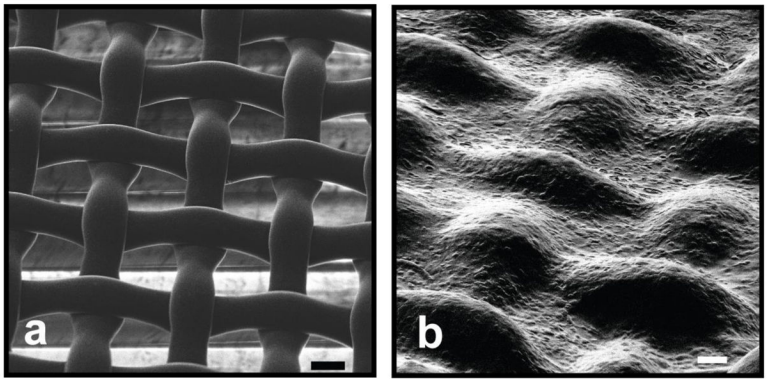

Figure 1.

Helium ion images of an a) uncoated nylon wound dressing and b) LbL-coated wound dressing. Growth factor-eluting films form continuous films that bridge the pores of the underlying woven nylon. Scale bars 20μm and 50μm respectively.

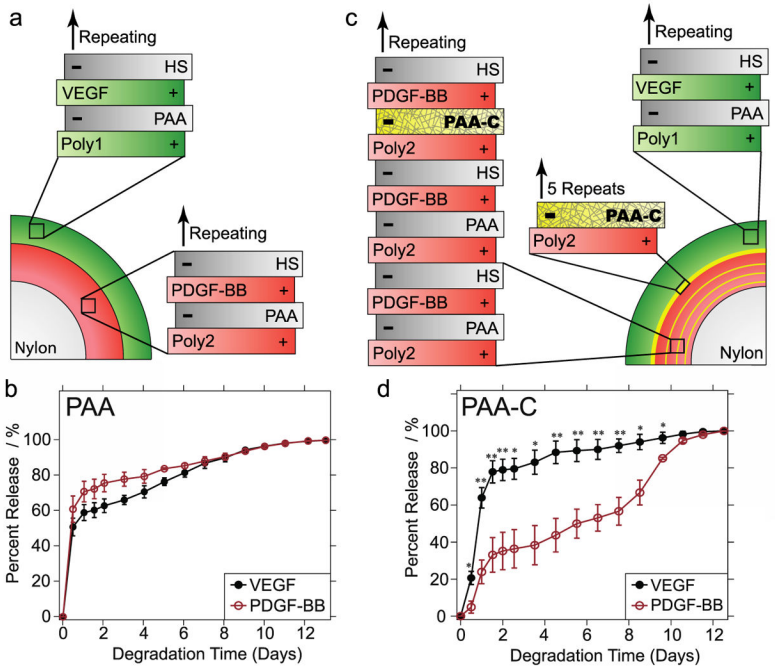

Figure 2.

a) Architecture of initial wound dressing. A PDGF-BB-containing film is deposited in contact with the nylon substrate. Subsequently, a VEGF-containing film is deposited on top of the PDGF-BB film. (b) Release profiles for VEGF and PDGF-BB for dressing architecture in part (a). (c) Architecture of dressing containing dithiol-crosslinked diffusion barriers. Periodic cysteine-modified PAA layers within the PDGF-BB section of the dressing reduce interfilm diffusion and enable independent control of release kinetics. (d) Release profiles for VEGF and PDGF-BB from dressing architecture shown in part (c). *, $p<0.05$; **, $p<0.01$ vs PDGF-BB release percent.

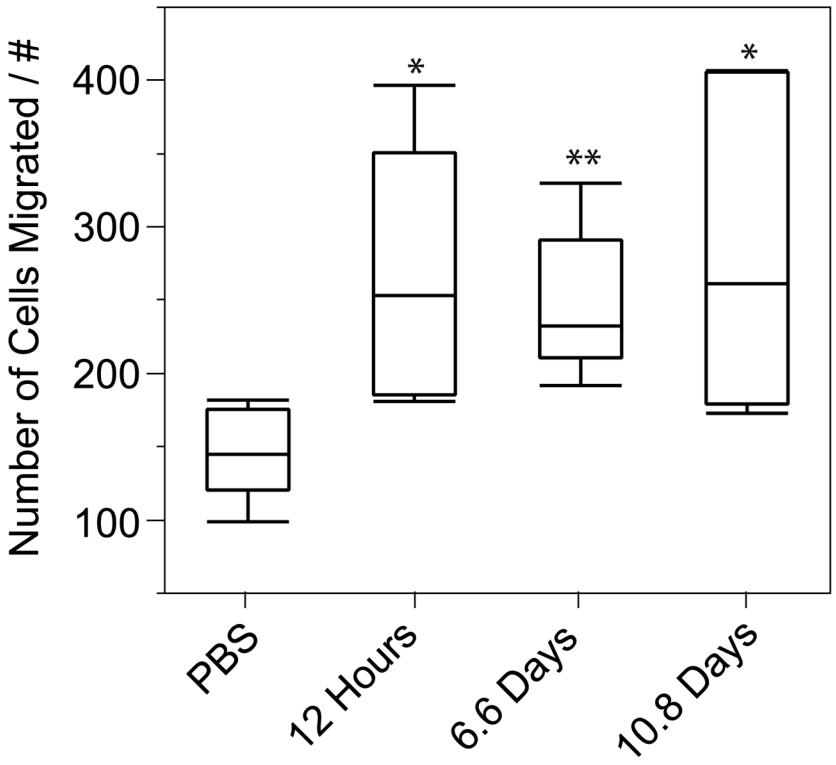

Figure 3.
Growth factors over the course of 11 days promote migration of human dermal fibroblasts. *, $p<0.05$; **, $p<0.005$. n=7–10.

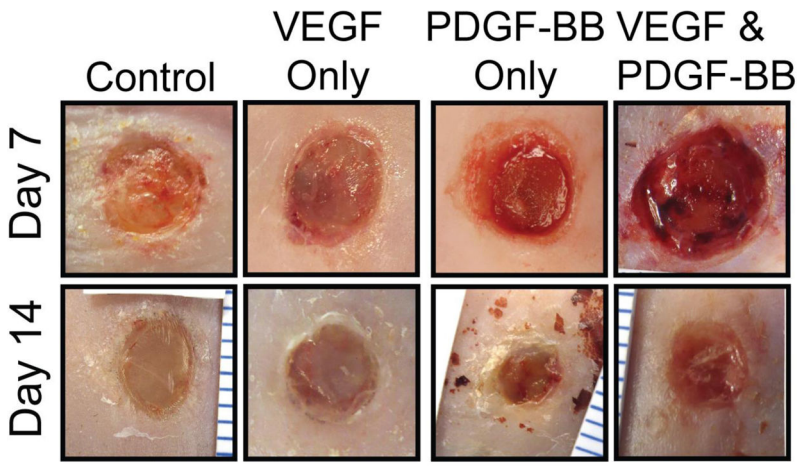

Figure 4.
Representative wound images of visual appearance at day 7 and day 14 for each treatment regimine.

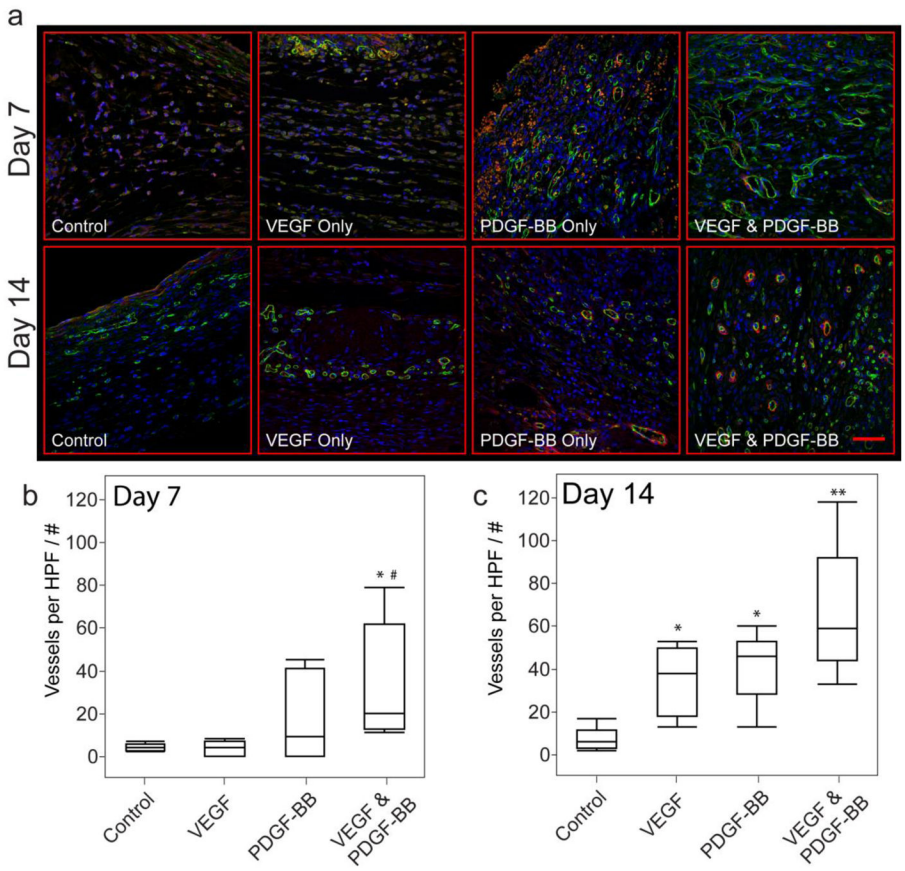

Figure 5.

(a) Immunofluorescence images of vessel growth for each treatment regime. Green: CD31; Red: α-smooth muscle actin; Blue: DAPI. Scale bar 50μm (b) Quantification of vessel density at day 7. (c) Quantification of vessel density at day 14. *, $p<0.01$ vs. control; **, $p<0.001$ vs. control; #, $p<0.05$ vs. VEGF.

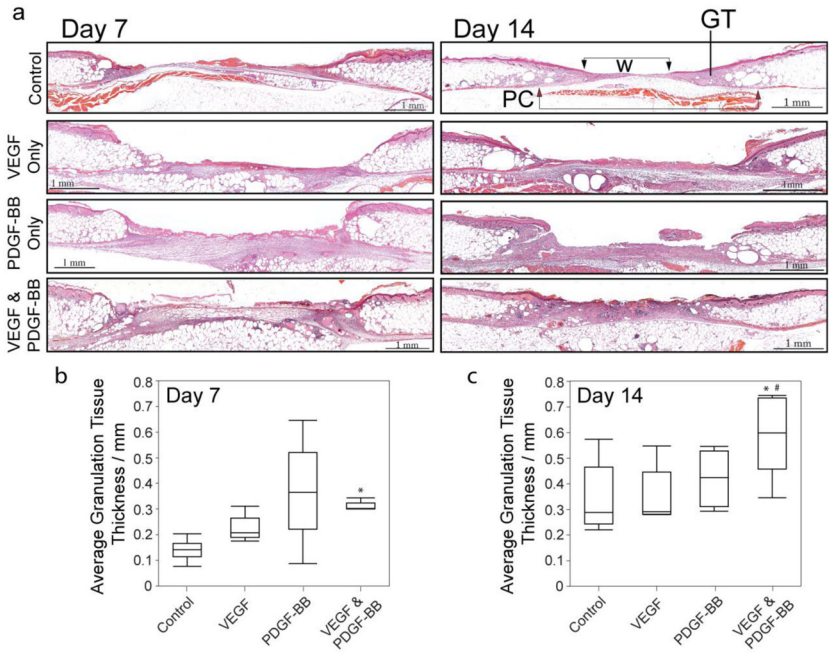

Figure 6.

(a) Representative histology sections (H&E stain). GT: Granulation Tissue; W: Wound Gap; PC: Panniculus Carnosus Gap. Average thickness of granulation tissue within wound bed at (b) day 7 and (c) day 14. *, $p < 0.05$ vs. control. #, $p<0.05$ vs. VEGF.

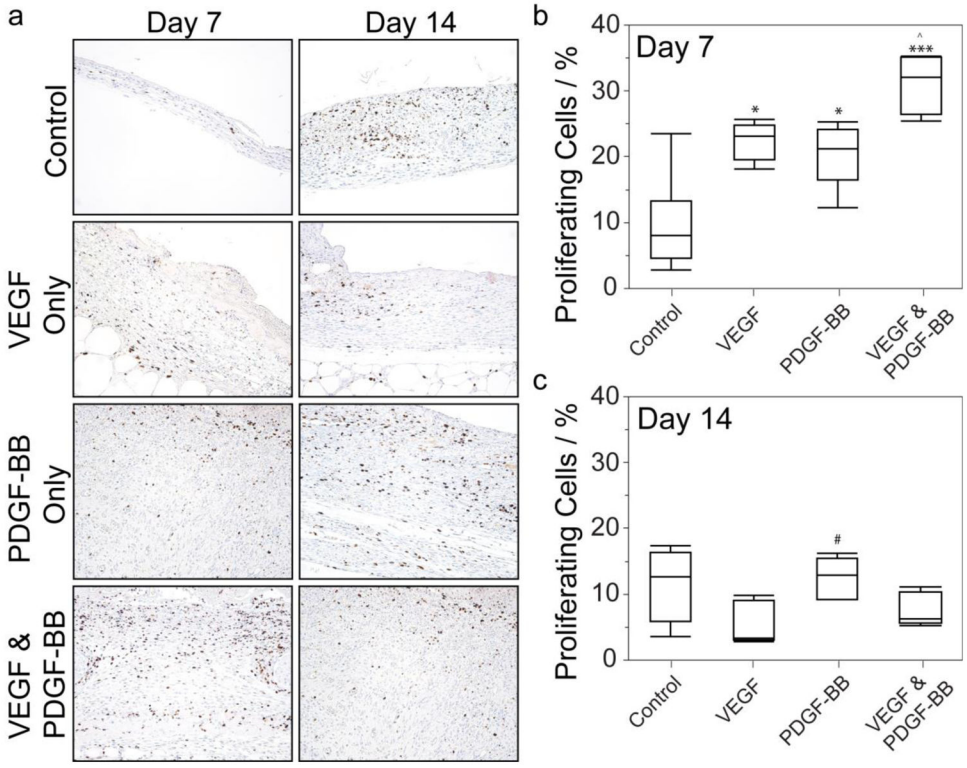

Figure 7.

Cellular proliferation in granulation tissue at day 7 and day 14. (a) Representative Ki-67 immunohistochemistry sections for each treatment regime at days 7 and 14. Fraction of proliferating cells in granulation tissue at (b) day 7 and (c) day 14. *, $p<0.05$ vs. control; ***, $p<0.0001$ vs. control; ^, $p<0.05$ vs. PDGF-BB; #, $P<0.05$ vs VEGF.

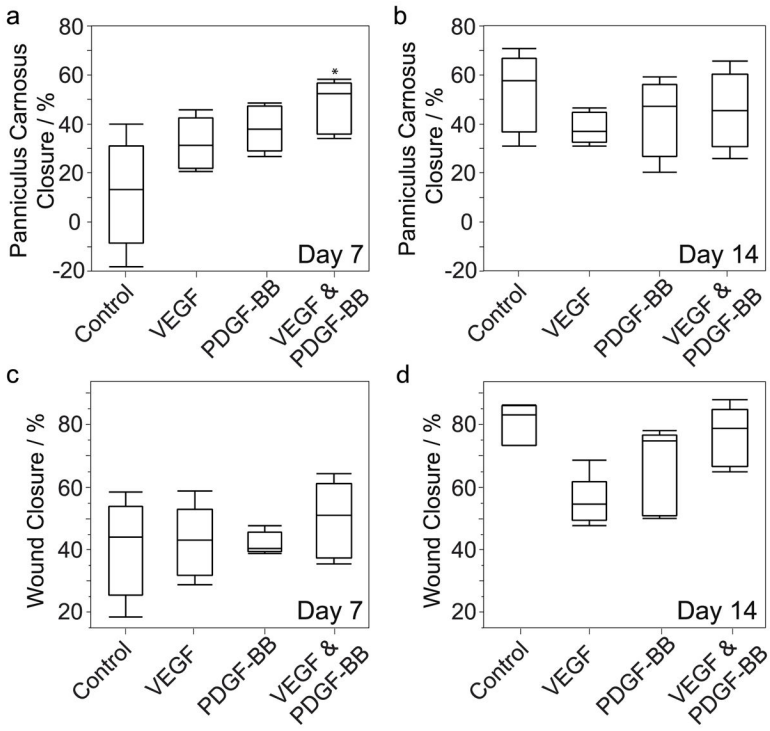

Figure 8.

Closure of the panniculus carnosus at (a) day 7 and (b) day 14. (c,d) Overall wound closure at day 7 and 14, respectively. *, $p<0.05$ vs. control.

Table 1

Total protein release from various dressing architectures. Total release from dressings with only PAA and those containing periodic PAAC are not statistically different, whereas dressings with only PAAC have minimal protein release out to 14 days (italics: $p<0.05$ vs. PAA & PAA+PAAC).

Dressing Architecture	Total VEGF Release at Day 14	Total PDGF Release at Day 14
PAA	238±50.5 ng/cm^2	170.3±59.9 ng/cm^2
PAA + Periodic PAAC	338.4±76.7 ng/cm^2	156.9±53.1 ng/cm^2
PAAC	*21.6±14.6 ng/cm^2*	*10.7±3.5 ng/cm^2*

Table 2

Ratio of thick to thin collagen at days 7 and 14.

Dressing Architecture	Collagen Fiber Thick/Thin Ratio at Day 7	Collagen Fiber Thick/Thin Ratio at Day 14
Control	4.8±3.8	13.2 ±2.8
VEGF Only	3.7±1.3	12.3±0.8
PDGF-BB Only	7.2±2.3	9.3±2.0
VEGF & PDGF-BB	3.0±0.6	11.9±6.6